

# Gamow-Teller strength distribution in proton-rich nucleus $^{57}\text{Zn}$ and its implications in astrophysics

Jameel-Un Nabi <sup>1</sup> • Muneeb-Ur Rahman

**Abstract** Gamow-Teller (GT) transitions play a pre-eminent role in the collapse of stellar core in the stages leading to a Type-II supernova. The microscopically calculated GT strength distributions from ground and excited states are used for the calculation of weak decay rates for the core-collapse supernova dynamics and for probing the concomitant nucleosynthesis problem. The B(GT) strength for  $^{57}\text{Zn}$  is calculated in the domain of proton-neutron Quasiparticle Random Phase Approximation (pn-QRPA) theory. No experimental insertions were made (as usually made in other pn-QRPA calculations of B(GT) strength function) to check the performance of the model for proton-rich nuclei. The calculated B(GT) strength distribution is in good agreement with measurements and shows differences with the earlier reported shell model calculation. The pn-QRPA model reproduced the measured low-lying strength for  $^{57}\text{Zn}$  better in comparison to the KB3G interaction used in the large-scale shell model calculation. The stellar weak rates are sensitive to the location and structure of these low-lying states in daughter  $^{57}\text{Cu}$ . The structure of  $^{57}\text{Cu}$  plays a sumptuous role in the nucleosynthesis of proton-rich nuclei. The primary mechanism for producing such nuclei is the rp-process and is believed to be important in the dynamics of the collapsing supermassive stars. Small changes in the binding and excitation energies can lead to significant modifications of the predictions for the synthesis of proton rich isotopes. The  $\beta^+$ -decay and electron capture (EC) rates

on  $^{57}\text{Zn}$  are compared to the seminal work of Fuller, Fowler and Newman (FFN). The pn-QRPA calculated  $\beta^+$ -decay rates are generally in good agreement with the FFN calculation. However at high stellar temperatures the calculated  $\beta^+$ -decay rates are almost half of FFN rates. On the other hand, for rp-process conditions, the calculated electron capture ( $\beta^+$ -decay) rates are bigger than FFN rates by more than a factor 2 (1.5) and may have interesting astrophysical consequences.

**Keywords** weak-interaction rates; electron capture and beta decay, pn-QRPA theory; GT strength distribution, rp-process.

## 1 Introduction

The weak interactions and gravity are the guru that drive the evolution of heavy mass stars and the concomitant nucleosynthesis, which has been the subject of much computation. The incarnation of the core-collapse mechanism is the conversion of a fraction of the gravitational energy into kinetic energy of the ejecta and internal energy of the inner core of the exploding star (1). This inner core is mainly composed of iron group nuclei and when this inner core exceeds the appropriate Chandrasekhar mass limits it becomes unstable and inaugurates the implosion of the inner core and consequently announces the death of the star in a catastrophic explosion. The relic is either a neutron star or black hole depending on the mass of the progenitors. If the stars are not too massive then they collapse and consequently bounce and explode in spectacular visual display commonly known as type-II or Ib/c supernovae. The collapse of the star is very sensitive to the entropy and to the number of leptons per baryon,  $Y_e$  (2; 3). The neutrinos are considered as main sink of energy and lepton number until the core density

Jameel-Un Nabi

Faculty of Engineering Sciences, GIK Institute of Engineering Sciences and Technology, Topi 23640, Swabi, Khyber Pakhtunkhwa, Pakistan

Muneeb-Ur Rahman

Department of Physics, Kohat University of Science and Technology, Kohat 26000, Khyber Pakhtunkhwa, Pakistan

<sup>1</sup>Corresponding author email : jameel@giki.edu.pk

reaches around  $10^{10} g - cm^{-3}$ . At later stage of the collapse this assumption is no longer legitimate as weak interaction rates increase with increase of stellar core density. For densities  $> 10^{11} g - cm^{-3}$ , the neutrinos mean free paths become shorter and consequently they proceed through all phases of free streaming, diffusion, and trapping. The most tightly bound of all the nuclei in the inner core of star is  $^{56}Fe$  (4) and further fusing of the nuclei is highly endothermic. The second bottleneck to the synthesis of heavier elements is the high  $Z$  number which poses high coulombic barrier for the charged particles to initiate nuclear reactions at stellar core temperatures. This impediment to further nucleosynthesis is rescinded with the help of neutron capture processes in the stellar core to form heavier isotopes beyond iron group nuclei. These processes are further classified into slow (s-) and rapid (r-) neutron capture processes depending on the neutron capture time scale  $\tau_n$  and beta decay time scale  $\tau_\beta$  for nucleus to endure beta decay. As discussed earlier that weak interaction and gravity are the mentor that drives the stellar evolutionary process and its subsequent death in a cataclysmic explosion. The main weak interaction processes that play an effective role in the stellar evolution are beta decays, electron and positron capture processes and neutrinos emission/capture processes subject to the physical conditions available for these processes in the stellar core. These weak decay processes are smitten by Fermi and Gamow-Teller (GT) transitions. Fermi transitions are straightforward and are important only for beta decays. For nuclei with  $N > Z$ , Fermi transitions are Pauli blocked and the GT transitions dominate and their calculation is model dependent. Spin-isospin-flip excitations in nuclei at vanishing momentum transfer are commonly known as GT transitions. These transitions are ideal probe to test nuclear structure and play preminent role in the nucleosynthetic origin of the elements in the late phases of the stellar life. When the stellar matter is degenerate then the phase space for the electron in beta decay is Pauli blocked and electron captures become dominant in the stellar core producing neutrinos which escape from the surface of the star and takes away the core energy and entropy as well. These electron capture rates and  $\beta^+$  decay rates are very sensitive to the distribution of the  $GT_+$  strength which is responsible for changing a proton into a neutron (the plus sign is for the isospin raising operator ( $t_+$ ), present in the GT matrix elements, which converts a proton into a neutron). The authors in (5; 6) took the accurate neutrino transport into account in their hydrodynamic studies of core-collapse supernovae and showed that the bulk of the neutrino-heated ejecta is proton-rich during the early phase ( $\leq 1s$ ). Their studies also provided

that it is likely possible that the neutrino-induced rp-process takes place in all core-collapse supernovae and other astrophysical sites such as collapsar jets or disk winds formed around a black hole. In reference (7) the authors discovered an extremely luminous X-ray outburst that marked the birth of a supernova of Type Ibc. They attributed the X-ray outburst to the break-out of the supernova shock-wave from the progenitor.

The open shell nuclei with a few nucleons outside a doubly magic shell closure are of colossal interest to test the nuclear model predictions.  $^{57}Cu$  is of paramount importance in this regard to test the pn-QRPA predictions. The  $pf$ -shell nucleus  $^{57}Cu$  has a single proton just above the closed core of even-even  $^{56}Ni$  with  $Z = N = 28$ . This simple structure permits far more accurate model calculations than are possible in the middle of a nuclear shell. In particular, a comparison of the low-lying levels of  $^{57}Cu$  with the well-determined excited states of its mirror nucleus  $^{57}Ni$  is important for studying the charge symmetry of the nucleus. The doubly magic nature of  $^{56}Ni$  confers it a stable structure and elements beyond  $^{56}Ni$  are cooked in the stellar pot only via  $^{56}Ni(p, \gamma)^{57}Cu$  reaction. The authors in Ref. (8) pointed out that the structure of  $^{57}Cu$  plays a sumptuous role in the nucleosynthesis of proton-rich nuclei. This points the fact that this reaction rate is susceptible to the structure of  $^{57}Cu$  and environs nuclei, including their binding energies. The primary mechanism for producing such nuclei is the rp-process and is believed to be important in the dynamics of the collapsing supermassive stars and x-ray bursts (9). The rp-process is characterized by proton capture reaction rates that are orders of magnitude faster than any other competing process, specially  $\beta$ -decay rates. The reaction path follows a series of fast (p, $\gamma$ )-reactions until further proton capture is inhibited, either by negative proton capture Q-values (proton decay) or small positive proton capture Q-values (photodisintegration). As electrons captures in the stellar pot assist the cooking process and gravity, therefore, it is crucial to know the nuclear structure properties of the doubly magic shell  $^{56}Ni$  and nuclei in its vicinity. These nuclei drive the electron capture processes in the dense core of heavy mass stars. The beta decay rate calculations require the evaluation of the GT strengths for many levels per nucleus. The pn-QRPA theory gives us the emancipation to use model space as big as  $7\hbar\omega$  rather than truncated model spaces usually employed in some shell model calculations.

Earlier the half-lives for  $\beta^+$ /EC decays for neutron-deficient nuclei with atomic numbers  $Z = 10 - 108$  were calculated up to the proton drip line for more than 2000 nuclei using the same model (10). These microscopic

calculations gave a remarkably good agreement with the then existing experimental data (within a factor of two for more than 73% of nuclei with experimental half-lives shorter than 1 s for  $\beta^+$ /EC decays). Most nuclei of interest of astrophysical importance are the ones far from stability and one has to rely on theoretical models to estimate their beta decay properties. The accuracy of the pn-QRPA model increases with increasing distance from the  $\beta$ -stability line (shorter half-lives) (10; 11). This is a promising feature with respect to the prediction of experimentally unknown half-lives (specially those present in the stellar interior), implying that the predictions are made on the basis of a realistic physical model.

Nucleosynthesis in proton-rich ejecta occur at low densities. At high densities the composition is neutron-rich. Under terrestrial conditions  $^{57}\text{Zn}$   $\beta^+$  decays to  $^{57}\text{Cu}$ . We used the calculated ground and excited state GT strength functions to microscopically calculate the  $\beta^+$ /EC rate of  $^{57}\text{Zn}$  in stellar matter. In proton-rich supernova environments  $^{57}\text{Zn}$  is produced at high temperatures where nuclear statistical equilibrium is valid. According to studies by authors in Ref. (8) the peak conditions for rp-process are in the vicinity of  $T = (1-3)$  GK and  $\rho = (10^6 - 10^7)$   $\text{gcm}^{-3}$ . The current analysis shows that the electron capture and positron decay rates of  $^{57}\text{Zn}$  contribute roughly equally to the total weak rates at peak rp-process conditions (with the positron decay rates bigger roughly by a factor of 6-7). At still higher temperatures and densities the electron capture on  $^{57}\text{Zn}$  dominates. As a result both  $\beta^+$  and electron capture stellar rates on  $^{57}\text{Zn}$  are being presented in this paper.

Section 2 describes the theoretical formalism of pn-QRPA calculation. Section 3 discusses the pn-QRPA calculated GT strength functions and its comparison with measurements and previous calculation. The calculated weak rates are presented in Section 4. Here we also compare our results with the pioneering calculation of Fuller and collaborators (12). We finally conclude our findings in Section 5.

## 2 Model Description

The nuclei involved in the stellar interior have finite probability of occupation of excited states and the state by state evaluation of the GT strength distribution from these excited states is a formidable task. The pn-QRPA is considered an efficient model to extract the GT strengths for the ground as well as excited states of the involved nuclei in stellar matter thanks to the huge available model space of seven major shells. The transitions from the excited states contribute effectively to

the total electron capture rate and a microscopic calculation of excited state GT strength distributions is desirable. The electron capture rates play a pivotal role in the dynamics of core collapse of stars. The pn-QRPA model is used in the present work to calculate the GT strength functions and associated electron capture/ $\beta^+$ -decay rates for proton-rich nucleus  $^{57}\text{Zn}$ .

The Hamiltonian of the pn-QRPA is given by

$$H^{\text{QRPA}} = H^{\text{sp}} + V^{\text{pair}} + V_{\text{GT}}^{\text{ph}} + V_{\text{GT}}^{\text{pp}}, \quad (1)$$

where  $H^{\text{sp}}$  is the single-particle Hamiltonian,  $V^{\text{pair}}$  is the pairing force,  $V_{\text{GT}}^{\text{ph}}$  is the particle-hole (ph) GT force, and  $V_{\text{GT}}^{\text{pp}}$  is the particle-particle (pp) GT force. Pairing is treated in the *BCS* approximation, where an assumed constant pairing force with force strength  $G$  ( $G_p$  and  $G_n$  for protons and neutrons, respectively) is applied,

$$V^{\text{pair}} = -G \sum_{jmj'm'} (-1)^{l+j-m} c_{jm}^+ c_{j-m}^+ (-1)^{l'+j'-m'} c_{j'-m'} c_{j'm'}, \quad (2)$$

where the sum over  $m$  and  $m'$  is restricted to  $m, m' > 0$ , and  $l$  donates the orbital angular momentum.

In the present work, in addition to the well known particle-hole GT force (13; 14; 15)

$$V_{\text{GT}}^{\text{ph}} = 2\chi \sum_{\mu} (-1)^{\mu} Y_{\mu} Y_{-\mu}^+, \quad (3)$$

with

$$Y_{\mu} = \sum_{j_p m_p j_n m_n} \langle j_p m_p | t_{-\sigma_{\mu}} | j_n m_n \rangle c_{j_p m_p}^+ c_{j_n m_n}, \quad (4)$$

the particle-particle GT force (16; 17)

$$V_{\text{GT}}^{\text{pp}} = -2\kappa \sum_{\mu} (-1)^{\mu} P_{\mu}^+ P_{-\mu}, \quad (5)$$

with

$$P_{\mu}^+ = \sum_{j_p m_p j_n m_n} \langle j_n m_n | (t_{-\sigma_{\mu}})^+ | j_p m_p \rangle (-1)^{l_n + j_n - m_n} c_{j_p m_p}^+ c_{j_n - m_n}^+, \quad (6)$$

is also taken into account.

The capture/decay rate of a transition from the  $i$ th state of a parent nucleus ( $Z, N$ ) to the  $j$ th state of the daughter nucleus ( $Z-1, N+1$ ) is given by

$$\lambda_{ij} = \ln 2 \frac{f_{ij}(T, \rho, E_f)}{(ft)_{ij}}, \quad (7)$$

$f_{ij}$  is the phase space integral. The  $(ft)_{ij}$  of an ordinary  $\beta^{\pm}$  decay from the state  $|i\rangle$  of the mother nucleus

to the state  $|f\rangle$  of the daughter is related to the reduced transition probability  $B_{ij}$  of the nuclear transition by

$$(ft)_{ij} = D/B_{ij}. \quad (8)$$

The  $D$  appearing in Eq. 8 is compound expression of physical constants,

$$D = \frac{2\pi^3 \hbar^7 \ln 2}{g_V^2 m_e^5 c^4}, \quad (9)$$

and the reduced transition probability of the nuclear transition is

$$B_{ij} = B(F)_{ij} + (g_A/g_V)^2 B(GT)_{ij}, \quad (10)$$

The value of  $D = 6146 \pm 6$  s (18) is adopted and the ratio of the axial-vector ( $g_A$ ) to the vector ( $g_V$ ) coupling constant is taken as -1.257.  $B(F)_{ij}$  and  $B(GT)_{ij}$  are reduced transition probabilities of the Fermi and GT transitions, respectively. These reduced transition probabilities of the nuclear transition are given by,

$$B(F)_{ij} = \frac{1}{2J_i + 1} |\langle j || \sum_k t_{\pm}^k || i \rangle|^2, \quad (11)$$

$$B(GT)_{ij} = \frac{1}{2J_i + 1} |\langle j || \sum_k t_{\pm}^k \bar{\sigma}^k || i \rangle|^2. \quad (12)$$

Calculation of phase space integrals can be seen from Ref. (19).

The number density of electrons associated with protons and nuclei is  $\rho Y_e N_A$ , where  $\rho$  is the baryon density,  $Y_e$  is the ratio of electron number to the baryon number, and  $N_A$  is the Avogadro's number.

$$\rho Y_e = \frac{1}{\pi^2 N_A} \left(\frac{m_e c}{\hbar}\right)^3 \int_0^\infty (G_- - G_+) p^2 dp, \quad (13)$$

where  $p = (w^2 - 1)^{1/2}$  is the electron or positron momentum.

The total capture/decay rate per unit time for a nucleus in thermal equilibrium at temperature  $T$  for any weak process is then given by

$$\lambda = \sum_{ij} P_i \lambda_{ij}. \quad (14)$$

Here  $P_i$  is the probability of occupation of parent excited states and follows the normal Boltzmann distribution. The summation over all initial and final states is carried out until satisfactory convergence in the rate calculations is achieved.

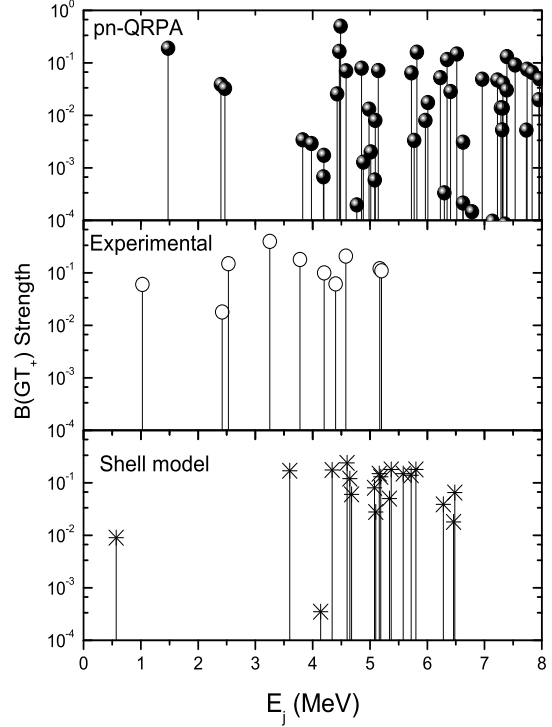


**Fig. 1** The comparison of pn-QRPA, experimental, and shell model  $B(GT_+)$  strength distribution of  $^{57}\text{Zn}$  as a function of  $^{57}\text{Cu}$  excitation energy.

### 3 Gamow-Teller Strength Distributions

The charge exchange reactions with high resolution are important probe for the study of nuclear structure in astrophysics. The GT strengths play an important role in electron capture and beta decay processes in the dynamics of stellar collapse (20; 21). Experimentally the (p, n), (n, p), (d, 2He), and (2He, t) reactions can be used to probe the GT transitions (in both directions) at higher excitation energies. Turning to theory one sees that a large amount of calculations of weak interaction rates for astrophysical applications have become available in recent times (e.g. (19; 22; 23; 24; 25)).

To allow the reader the judgment of quality achieved in the pn-QRPA model underlying the stellar weak interaction rate calculation, the  $B(GT)$  strength calculated using the pn-QRPA theory is compared with experimental (18) and with  $B(GT)$  strengths predictions obtained from a large-scale shell model calculation using the effective interaction KB3G (26). The results are depicted in Fig. 1. Vieira et al. (27) for the first time probed the structure of  $^{57}\text{Cu}$  in the beta decay of  $^{57}\text{Zn}$  by employing the  $^{40}\text{Ca}(^{20}\text{Ne}, 3n)$  fusion evaporation reaction and by Zhou et al. (28) in the  $^1\text{H}(^{58}\text{Ni},$

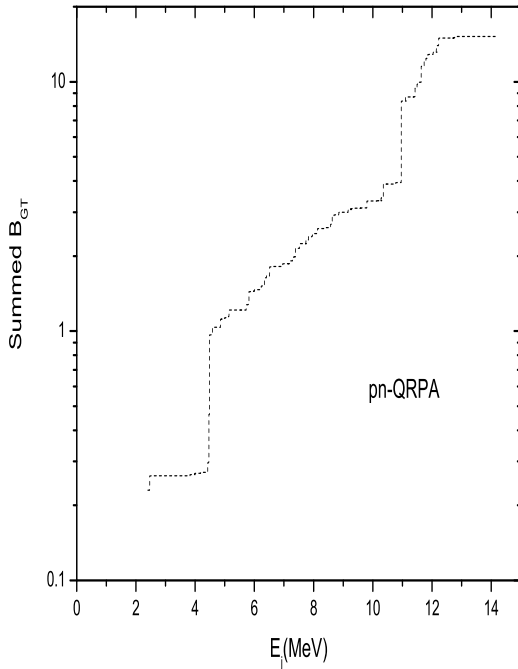


**Fig. 2** The pn-QRPA calculated integrated strength within the  $Q_{EC}$  window.  $E_j$  represents the energy in daughter nucleus  $^{57}\text{Cu}$  in units of MeV.

$^{57}\text{Cu}(\gamma)2n$  reaction by using the recoil mass spectrometer MARS at the Texas A&M Cyclotron Institute. Considerable improvements were obtained in Ref. (18) concerning the quality of the experimental data, in particular with respect to source purity and proton energy resolution.

The authors in Ref. (18) investigated the beta-delayed proton decay of  $^{57}\text{Zn}$  at GSI online isotope separator.  $^{57}\text{Zn}$  nuclei were produced in fusion evaporation reactions,  $^{28}\text{Si}(^{32}\text{S}, 3n)$ , by using a 150 MeV  $^{32}\text{S}$  beam on a  $^{28}\text{Si}$  target and then the beta-delayed protons were measured with high resolution by employing a charged-particle detector. The GT strength distributions observed in this experiment is shown in the middle panel of Fig. 1. The morphology of the pn-QRPA GT strength (upper panel) for beta transitions between the ground state of  $^{57}\text{Zn}$  to the ground state of daughter  $^{57}\text{Cu}$  is in good agreement with the measured data of Ref. (18). These transitions are of allowed nature in daughter  $^{57}\text{Cu}$ . The experimental GT strength between 2 and 3 MeV is well reproduced by pn-QRPA. These peaks were missing in the large-scale shell model calculation as shown in the bottom panel of Fig. 1. We

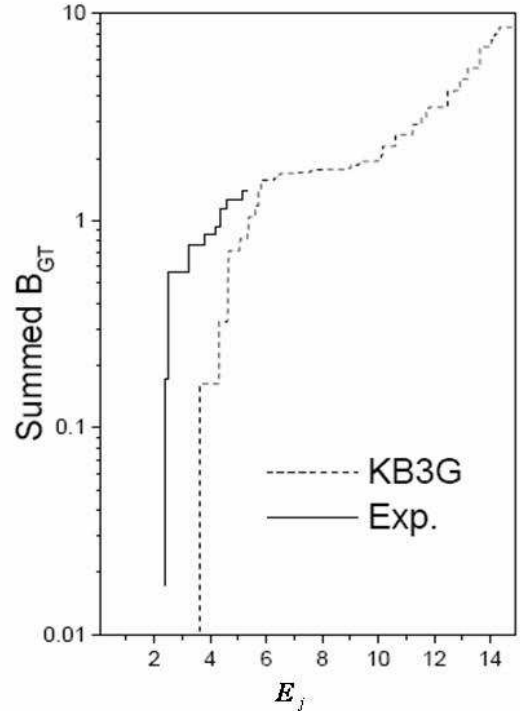


**Fig. 3** Comparison of experimental and shell model integrated GT strength within the  $Q_{EC}$  window. The figure is reproduced from Ref. (18).

used the  $Q$ -value of 14.51 MeV for  $^{57}\text{Zn}$  from the recent compilations of Ref. (29; 30).

It is evident that the GT strength distribution calculated by the shell model KB3G, as compared to pn-QRPA and experimental results, tends to shift to higher excitation energies in daughter  $^{57}\text{Cu}$ . The pn-QRPA integrated GT strength over the  $Q$  window is shown in Fig. 2. For comparison, the overall shift in  $B(\text{GT})$  strength of the shell model prediction along with the experimentally extracted integrated GT strength is shown in Fig. 3. In the present work we obtained a summed  $B(\text{GT})$  of 1.86 as compared to 1.25 in Ref. (18) within the excitation energy interval between 0 and 7 MeV in daughter  $^{57}\text{Cu}$ . The authors in Ref. (18) increased the strength by the upper  $B(\text{GT})$  limit for the 1.028 MeV state and the theoretical  $B(\text{GT})$  value for the IAS to yield  $1.44^{+0.25}_{-0.17}$  and they estimated that less than 2% of the total GT strength could be missed due to the unobserved gamma-transitions. The shell model predicted strength for the same excitation of energies amounts to 1.68.

In beta decay experiments the sensitivity of the experiment strongly decreases as one moves to higher excitation energies in daughter. This puts a limit for

such experiments and thus one can only probe the low-energy tails of the GT strength distribution. Consequently one has to rely on theoretical models for the calculation of GT strength distributions in high excitation energies region as well as for parent excited states. Within the  $Q$  window of the reaction, we extracted a total GT strength of 15.23 and the KB3G calculation amount it to be 8.63. The pn-QRPA results include a quenching factor of 0.8 as usually employed for the  $pf$ -shell nuclei. The luxurious  $7\hbar\omega$  model space of the pn-QRPA facilitates one to extract the state by state evaluation of the these GT strength for higher excited states as well without assuming the Brink's hypothesis and model space truncation as usually employed in the shell model calculations. The truncation level, i.e, the number of nucleons which are to be excited from the  $f_{7/2}$  orbital to the rest of the  $pf$ -shell, in the KB3G calculation was restricted to 4 nucleons for parent  $^{57}\text{Zn}$  and 5 nucleons for daughter  $^{57}\text{Cu}$ . The pn-QRPA model extracted a bigger total strength as compared to the KB3G interactions employed in the shell model calculation. This certainly affects the calculation of  $\beta^+$ -decay and electron capture rates in the stellar core at high densities. Except at higher temperatures, the double shell closure of  $^{56}\text{Ni}$  confers it stability compared to any of its neighbors and the main path of the rp-process passes through  $^{56}\text{Ni}$ . These properties pointed to the fact that heavier nuclei may be produced by the rate of the radiative proton capture reaction  $^{56}\text{Ni}(p, \gamma)^{57}\text{Cu}$  and confirm the candidature of  $^{56}\text{Ni}$  as a waiting point nucleus in the reaction network. The rate of this reaction in the stellar kilns is due almost entirely to the first four resonances (28) and particularly very sensitive to the location and structure of the low-lying states in daughter  $^{57}\text{Cu}$ . The pn-QRPA accounted well for these low-lying states in  $^{57}\text{Cu}$ . The proton separation energy of  $^{57}\text{Cu}$  is merely  $S_p = 694.87$  keV (29; 30), and so all of its excited states are resonances in this reaction. The authors in Ref. (28) stressed that small changes in the binding and excitation energies lead to significant modifications of the predictions for the synthesis of proton rich isotopes with  $A > 56$  and possibly for the time evolution of cosmic x-ray bursts.

We calculated the ground state and excited states GT strength functions of  $^{57}\text{Zn}$  using the pn-QRPA model. The calculation was performed for a total of 259 excited states in  $^{57}\text{Zn}$  covering an excitation energy of around 30 MeV. The density of states were chosen accordingly and contributions to GT strength from all excited states were incorporated in the rate calculation. The ASCII files of these GT strength functions are available and can be requested from the corresponding author.

#### 4 $\beta^+$ -Decay and Electron Capture Rates

At low stellar densities and temperatures,  $\beta^+$ -decay is the dominant mode for  $^{57}\text{Zn}$  to transform to  $^{57}\text{Cu}$ . For the calculation of the stellar weak interaction rate under corresponding physical conditions, it is of colossal importance to reproduce the measured GT strength distribution as compared to the total GT strength due to very strong energy dependence of the phase space factors. As discussed earlier the pn-QRPA model reproduced the low-lying strength for  $^{57}\text{Zn}$  better in comparison to the KB3G interaction used in the large shell model calculation. The stellar weak rates are sensitive to the location and structure of these low-lying states in daughter  $^{57}\text{Cu}$ . At the lowest temperature considered in this work ( $T_9[K] = 0.01$ ), excited parent states are not appreciably populated (where  $T_9$  is the stellar temperature in units of  $10^9 K$ ), while at low density ( $\rho Y_e = 10 \text{ gcm}^{-3}$ ), the continuum electron density is quite low and the stellar rates should be close to the terrestrial values. At this value of temperature and density the calculated half-life for  $\beta^+$ -decay on  $^{57}\text{Zn}$  is 39.6 ms which is in excellent agreement with the measured value of 40 ms (27).

Table 1 shows the calculated  $\beta^+$ -decay rates on  $^{57}\text{Zn}$  as a function of stellar temperature and density. In Table 1 the first column gives the stellar density in units of  $\text{gcm}^{-3}$ . The second column gives the value of temperature in units of  $10^9 K$ . The third column gives the value of the calculated  $\beta^+$ -decay rates in units of  $\text{sec}^{-1}$  whereas the final column shows the ratio of the calculated  $\beta^+$ -decay rates to the electron capture rates for physical conditions given in first two columns. One should note that even though terrestrially  $^{57}\text{Zn}$   $\beta^+$ -decays to  $^{57}\text{Cu}$  with a 100% ratio (no electron capture), we do calculate a finite ratio of  $\beta^+$ -decay to electron capture even at low temperature and density (see Table 1). This is because we calculate only continuum electron capture and no bound states capture. It can be seen from the table that there is no appreciable change in the  $\beta^+$ -decay rates as the core stiffens from low density to high density region. However the rates increase considerably with increasing stellar temperature due to a considerable increase in the available phase space. At the later stages of the collapse,  $\beta^+$ -decay becomes unimportant as an increased electron chemical potential, which grows like  $\rho^{1/3}$  during in fall, drastically reduces the phase space. These results in increased electron capture rates during the collapse phase. Electron capture rates on  $^{57}\text{Zn}$  hence become important during the very late phases of stellar evolution of massive stars (prior to collapse) and at high stellar temperatures. At  $\rho Y_e[\text{gcm}^{-3}] = 10^{11}$  the calculated electron capture rates

**Table 1**  $\beta^+$ -decay rates (in units of  $\text{sec}^{-1}$ ) and ratio of  $\beta^+$ -decay to electron capture rates on  $^{57}\text{Zn}$  for different selected densities and temperatures in stellar matter.  $\rho Y_e$  denotes the stellar density in units of  $g/\text{cm}^3$  and  $T_9$  represents the temperature in  $10^9$  K.

$\rho Y_e$	$T_9$	$\lambda_{\beta^+}$	$R(\beta^+/EC)$	$\rho Y_e$	$T_9$	$\lambda_{\beta^+}$	$R(\beta^+/EC)$
10	0.01	17.50	5.6E+05	$10^7$	0.01	17.50	6.5E+00
10	1	19.54	5.8E+04	$10^7$	1	19.54	7.0E+00
10	3	21.09	1.8E+02	$10^7$	3	21.09	7.0E+00
10	5	22.18	2.7E+01	$10^7$	5	22.23	6.4E+00
10	10	26.67	2.4E+00	$10^7$	10	26.73	1.9E+00
10	30	137.09	1.3E-01	$10^7$	30	137.09	1.3E-01
$10^3$	0.01	17.50	7.9E+03	$10^9$	0.01	17.50	3.5E-02
$10^3$	1	19.54	3.4E+04	$10^9$	1	19.54	3.8E-02
$10^3$	3	21.09	1.8E+02	$10^9$	3	21.09	3.9E-02
$10^3$	5	22.18	2.7E+01	$10^9$	5	22.28	4.0E-02
$10^3$	10	26.67	2.4E+00	$10^9$	10	27.10	4.1E-02
$10^3$	30	137.09	1.3E-01	$10^9$	30	143.88	6.7E-02
$10^5$	0.01	17.50	3.2E+02	$10^{11}$	0.01	17.50	5.8E-05
$10^5$	1	19.54	5.4E+02	$10^{11}$	1	19.54	6.4E-05
$10^5$	3	21.09	1.6E+02	$10^{11}$	3	21.09	6.8E-05
$10^5$	5	22.23	2.7E+01	$10^{11}$	5	22.28	7.1E-05
$10^5$	10	26.67	2.4E+00	$10^{11}$	10	27.10	8.3E-05
$10^5$	30	137.09	1.3E-01	$10^{11}$	30	151.36	4.0E-04

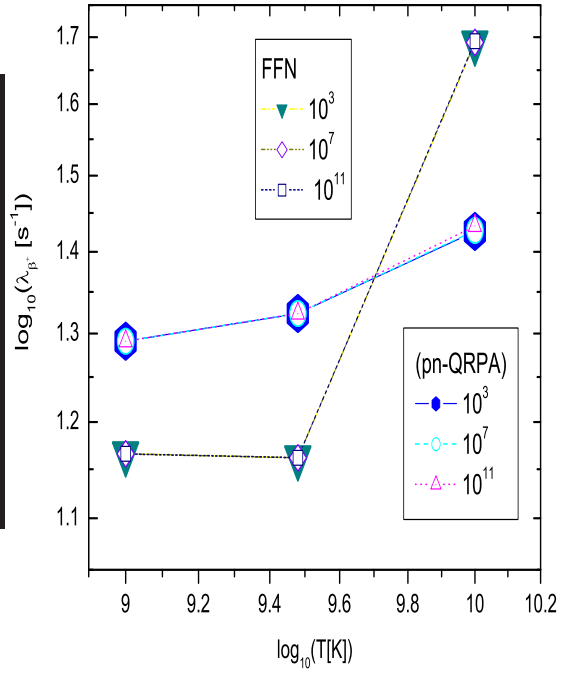


**Fig. 4** (Color on line) Comparison of the pn-QRPA and FFN (12)  $\beta^+$  decay rates of  $^{57}\text{Zn}$  nucleus as a function of temperature for selected densities (in units of  $g.\text{cm}^{-3}$  shown in legends) in stellar matter.

are bigger than the competing  $\beta^+$ -decay rates by more than four orders of magnitude. For the relevant peak rp-process conditions ( $T_9[K] \sim 3$  and  $\rho \sim 10^7$   $\text{gcm}^{-3}$ ), the pn-QRPA calculated  $\beta^+$ -decay rates are around a factor seven bigger than the corresponding electron capture rates. Therefore we present our results for both  $\beta^+$ -decay rates of  $^{57}\text{Zn}$  and electron capture rates on  $^{57}\text{Zn}$  and compare them with previous calculations.

To the best of author's knowledge, there are no shell model weak rates available in the literature for  $^{57}\text{Zn}$  nucleus. Therefore, pn-QRPA rates were compared with the pioneer work of Fuller et al. (12). This comparison for the  $\beta^+$  decay and electron capture rates are shown in Fig. 4, and Fig. 5, respectively. Fig. 4 shows that the pn-QRPA  $\beta^+$  decay rates are in good comparison with the FFN rates. However at high stellar temperatures ( $T_9[K] = 30$ ) the FFN rates are almost twice the calculated rates. The authors in Ref. (12) put no constraints on the threshold values of parent excitation energies while in the present calculation such constraints were incorporated through particle emission processes

(25) which lead to the suppression of pn-QRPA  $\beta^+$  decay rates at high stellar temperatures (when the probability of occupation of high-lying parent excited states increases substantially). Regarding the calculation of electron capture rates (Fig. 5) one notes that at high stellar densities (where electron capture rates surpass the  $\beta^+$  decay rates),  $\rho Y_e[\text{gcm}^{-3}] \sim 10^{11}$ , the FFN rates are in good comparison with the pn-QRPA electron capture rates. At lower densities the pn-QRPA electron capture rates are bigger by a factor 2 ( $T_9[K] \sim 1$ ) to a factor of 3 when  $T_9[K] = 30$ . This enhancement is attributed to the low placement of the GT centroid in the daughter nucleus,  $^{57}\text{Cu}$ , by the pn-QRPA model.

The  $\beta^+$ -decay and electron capture rates on  $^{57}\text{Zn}$  were calculated on a fine grid temperature-density scale suitable for simulation codes and for necessary interpolation purposes. The ASCII files of these rates may be requested from the corresponding author.

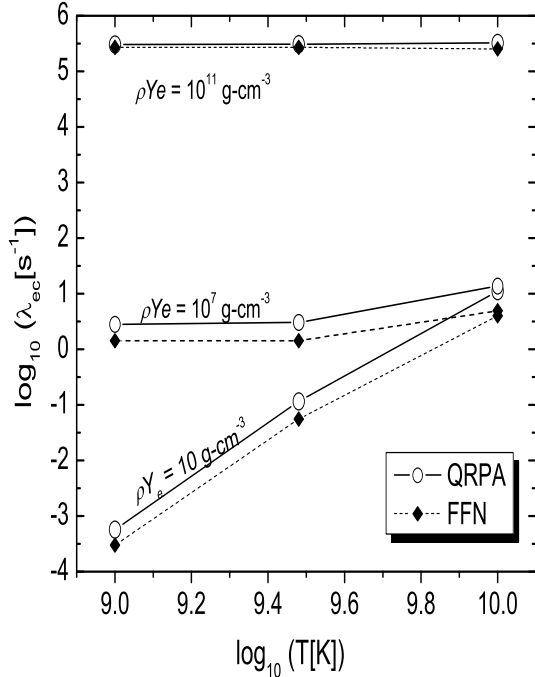


**Fig. 5** Comparison of the pn-QRPA and FFN (12) electron capture rates on  $^{57}\text{Zn}$  nucleus as a function of temperature for selected densities in stellar matter.

## 5 Summary

The GT strength function is an important ingredient in the complex dynamics of presupernova and supernova explosion since these GT transitions partly determine the  $\beta^+$ -decay and electron capture rates in the stellar core. The GT strength distributions in  $^{57}\text{Zn}$  were calculated within the domain of the pn-QRPA theory. The pn-QRPA calculated GT strength showed differences with the earlier reported shell model calculation. The pn-QRPA results for  $^{57}\text{Zn}$  were in good agreement with the experimental results (18) and reproduced well the measured GT strength between 2-3 MeV. The stellar weak decay rates are sensitive to the location and structure of these low-lying states in daughter  $^{57}\text{Cu}$ . Small changes in the binding and excitation energies can lead to significant modifications of the predictions for the synthesis of proton-rich isotopes. The primary mechanism for the production of the proton-rich nuclei is the rp-process and is believed to be important in the dynamics of the collapsing supermassive stars. The good agreement of the reported low-lying GT strength with the experimental results validates the choice of the

pn-QRPA theory as a preferred model for the calculation of weak rates for proton-rich nuclei. The choice of nuclear model can affect the prediction and synthesis of proton-rich isotopes as well as the time evolution of the cosmic x-ray burst and dynamics of the collapsing supermassive stars. For comparison, in the present work we obtained a summed  $B(\text{GT})$  of 1.86 as compared to 1.25 in Ref. (18) within the excitation energy interval between 0 and 7 MeV in daughter  $^{57}\text{Cu}$ . The shell model predicted strength for the same excitation energies amounts to 1.68.

The calculated GT strength functions were further used to calculate electron capture and  $\beta^+$ -decay rates of  $^{57}\text{Zn}$  in stellar matter, particularly for rp-process conditions. At high stellar temperatures the calculated  $\beta^+$ -decay rates on  $^{57}\text{Zn}$  are half of the corresponding FFN calculated rates. For typical peak rp-process conditions,  $T_9[\text{K}] \sim 3$  and  $\rho \sim 10^7 \text{ g cm}^{-3}$ , the pn-QRPA calculated  $\beta^+$ -decay (electron capture) rates on  $^{57}\text{Zn}$  are bigger by a factor of 1.5 (2). This may have interesting astrophysical consequences for collapse simulators.

Realistically speaking weak interaction mediated rates of hundreds of nuclei are involved in the complex dynamics of supernova explosion. Incidentally, the most abundant nuclei tend to have small weak rates as they are more stable and the most reactive nuclei tend to be present in minor quantities. Thus, the most important in the stellar core is the rate times abundance of a particular specie. We are in the process to calculate microscopically the weak decay rates for nuclei which are considered to be important in astrophysical environment as part of this on-going project. Few of such important weak rates were recently presented (e.g. (31; 32; 33; 34; 35; 36)). Work is still in progress for the microscopic calculation of weak rates of remaining key iron-regime nuclei. Core-collapse simulators are urged to test run the pn-QRPA reported weak rates in typical stellar conditions to check for probable interesting outcomes.

## References

- Burrows A., Livne E., Dessart L., Ott C. D., Murphy J.: Features of the acoustic mechanism of core-collapse supernova explosions. *Astrophys. J.* **640**, 878-890 (2006)
- Nabi J.-Un, Rahman M.-Ur.: Gamow-Teller Strength Distributions and Electron Capture Rates for  $^{55}\text{Co}$  and  $^{56}\text{Ni}$ . *Phys. Lett.* **B612**, 190 (2005)
- Bethe H.A., Brown G.E., Applegate J., Lattimer J.M.: Equation Of State In The Gravitational Collapse Of Stars. *Nucl. Phys.* **A324**, 487 (1979)
- Cowan J. J., Thielemann F.-K.: R-process nucleosynthesis in supernovae. *Phys. Today*, **57**, 47 (2004)
- Wanaajo S.: The rp-process in neutrino-driven winds. *Astrophys. J.* **647**, 1323 (2006)
- Kitaura F. S., Janka H.-Th., Hillebrandt W.: Explosions of O-Ne-Mg cores, the Crab supernova, and subluminal Type II-P supernovae. *Astron. and Astrophys.* **450**, 345 (2006)
- Soderberg A. M. et al.: An extremely luminous X-ray outburst at the birth of a supernova. *Nature* **453**, 469 (2008)
- Schatz H., Aprahamian A., Grzes J., Wiescher M., Rauscher T., Rembes J. F., Thielemann F.-K., Pfeiffer B., Möller P., Kratz K.-L., Herndl H., Brown B. A., Rebel H.: rp-process nucleosynthesis at extreme temperature and density conditions. *Phys. Rep.* **294**, 167 (1998)
- Wallace R. K., Woosley S. E.: Explosive hydrogen burning. *Astrophys. J. Suppl. Ser.* **45**, 389 (1981)
- Hirsch M., Staudt A., Muto K., Klapdor-Kleingrothaus H.V.: Microscopic Predictions of  $\beta^+$ /EC-Decay Half-Lives. *At. Data Nucl. Data Tables* **53**, 165 (1993)
- Staudt A., Bender E., Muto K., Klapdor-Kleingrothaus H.V.: Second-Generation Microscopic Predictions of Beta-Decay Half-lives of Neutron-Rich Nuclei. *At. Data Nucl. Data Tables* **44**, 79 (1990)
- Fuller G. M., Fowler W. A., Newman M. J.: Stellar Weak Interaction Rates for Intermediate Mass Nuclei. III. Rate Tables for the Free Nucleons and Nuclei with  $A = 21$  to  $A = 60$ . *Astrophys. J. Suppl. Ser.* **48**, 279 (1982)
- Halbleib J. A., Sorensen R. A.: Gamow-Teller beta decay in heavy spherical nuclei and the unlike particle-hole rpa. *Nucl. Phys.* **A98**, 542 (1967)
- Staudt A., Hirsch M., Muto K., Klapdor-Kleingrothaus H. V.: Calculation of  $\beta$ -delayed fission of  $^{180}\text{Tl}$  and application of the quasiparticle random-phase approximation to the prediction of  $\beta^+$ -decay half-lives of neutron-deficient isotopes. *Phys. Rev. Lett.* **65**, 1543 (1990)
- Muto K., Bender E., Oda T., Klapdor-Kleingrothaus H. V.: Proton-neutron quasiparticle RPA with separable Gamow-Teller forces. *Z. Phys. A* **341**, 407 (1992)
- Soloviev V. G.: Fragmentation of single-particle and collective motions in the quasiparticle-phonon nuclear model. *Prog. Part. Nucl. Phys.* **19**, 107 (1987)
- Kuzmin V. A., Soloviev V. G.: Gamow-Teller  $\beta^+$  decays and strength functions of (n, p) transitions in spherical nuclei. *Nucl. Phys.* **A486**, 118 (1988)
- Jokinen A. et al.: Beta decay of  $^{57}\text{Zn}$ . *Euro. Phys. J. Direct A* **3**, 1 (2002)
- Nabi J.-Un, Klapdor-Kleingrothaus H.V.: Weak Interaction Rates of sd-Shell Nuclei in Stellar Environments Calculated in the Proton-Neutron Quasiparticle Random-Phase Approximation. *At. Data Nucl. Data Tables* **71**, 149 (1999)
- Nabi J.-Un, Rahman M.-Ur.: Gamow-Teller Transitions from  $^{24}\text{Mg}$  and Their Impact on the Electron Capture Rates in the O+Ne+Mg Cores of Stars. *Phys. Rev.* **C75**, 035803 (2007)
- Fujita Y. et al.: Gamow-Teller strengths in proton-rich exotic nuclei deduced in the combined analysis of mirror transitions. *Phys. Rev. Lett.* **95**, 212501 (2005)
- Heger A., Woosley S.E., Martínez-Pinedo G., Langanke K.: Presupernova Evolution with Improved Rates for Weak Interactions. *Astrophys. J.* **560**, 307 (2001)
- Langanke K., Martínez-Pinedo G.: Rate tables for the weak processes of pf-shell nuclei in stellar environments. *At. Data Nucl. Data Tables* **79**, 1-46 (2001)
- Rahman M.-U.: The Gamow-Teller strength distributions and associated weak decay rates in stellar matter. PhD Thesis, 2007, GIK Institute of Engg. Sciences & Tech. Pakistan
- Nabi J.-Un, Klapdor-Kleingrothaus H.V.: Microscopic Calculations of Stellar Weak Interaction Rates and Energy Losses for fp- and fpg-Shell Nuclei. *At. Data Nucl. Data Tables* **88**, 237 (2004)
- Poves A., Sanchez-Solano ., Caurier E., Nowacki F.: Shell model study of the isobaric chains  $A=50$ ,  $A=51$  and  $A=52$ . *Nucl. Phys.* **A694**, 157 (2001)
- Vieira D. J., Sherman D. F., Zisman M. S., Gough R. A., Cerny J.: Extension of the  $T_z = 3/2$  beta-delayed proton precursor series to  $^{57}\text{Zn}$ . *Phys. Lett.* **B 60**, 261 (1976)
- Zhou X. G., Dejbakhsh H., Gagliardi C. A., Jiang J., Trache L., Tribble R. E.: Low-lying levels in  $^{57}\text{Cu}$  and the rp process. *Phys. Rev.* **C53**, 982 (1996)
- Audi G., Bersillon O., Blachot J., Wapstra A. H.: The NUBASE evaluation of nuclear and decay properties. *Nucl. Phys.* **A729**, 3 (2003)
- Audi G., Wapstra A. H., Thibault C.: The AME2003 Atomic Mass Evaluation (II). Tables, Graphs and References. *Nucl. Phys.* **A729**, 337 (2003)
- Nabi J.-Un, Sajjad M.: Neutrino Energy Loss Rates and Positron Capture Rates on  $^{55}\text{Co}$  for Presupernova and Supernova Physics. *Phys. Rev.* **C77**, 055802 (2008)
- Nabi J.-Un: Stellar neutrino energy loss rates due to  $^{24}\text{Mg}$  for O+Ne+Mg core simulations. *Phys. Rev.* **C78**, 045801 (2008)
- Nabi J.-Un.: Weak-Interaction-Mediated Rates on Iron Isotopes for Presupernova Evolution of Massive Stars. *Eur. Phys. J. A* **40**, 223 (2009)
- Nabi J.-Un.: Neutrino and antineutrino energy loss rates in massive stars due to isotopes of titanium. *Int. J. Mod. Phys. E* **19**, 1 (2010)
- Nabi J.-Un.: Expanded calculation of neutrino cooling rates due to  $^{56}\text{Ni}$  in stellar matter. *Phys. Scripta* **81**, 025901 (2010)
- Nabi J.-Un.: Stellar  $\beta^\pm$  decay rates of iron isotopes and its implications in astrophysics. *Adv. Space Res.* doi:10.1016/j.asr.2010.05.026 (2010)